



**International Nuclear Safety Center
of Russian Minatom**



**RELAP5/MOD3.2 ANALYSIS of KS FACILITY EXPERIMENTS on RBMK-1500
CORE THERMAL HYDRAULIC PROCESSES under PRESSURE HEADER BREAK
CONDITIONS PERFORMED in RUSSIAN RESEARCH CENTER
“KURCHATOV INSTITUTE”**

Authors: Vinogradov V.A., Balykin A.Yu.

(Company: Russian Research Centre “Kurchatov Institute”

Mailing address: Russia, 123182 Moscow, Kurchatov sq. 1

E-mail: vav@vver.kiae.ru

Phone: +7(095) 196-92-71

Fax: +7(095) 196-61-72

1. BACKGROUND AND INTRODUCTION

The purpose of validation calculations presented in the Analysis Report is an assessment of RELAP5/MOD3.2 suitability for description of thermal and hydraulic processes, which occur under specific conditions of RBMK type reactor during the accident with pressure header rupture and subsequent ECCS water injection. Calculation study was performed according to RELAP5/MOD3.2 validation plan for application to RBMK [1] developed by INSC in the framework of US INSC project # 6 “Computer Code Validation for VVER and RBMK”. At this project stage, 7 standard problems were included into the Code validation plan for RBMK. With regard to the readiness for analysis, there was INSCSP-R2 standard problem formulated in RRC KI “Investigation on thermohydraulic processes in the core of the RBMK type reactor at pressure header rupture performed on the KS test facility at RRC “Kurchatov Institute” [2]. This standard problem addresses phenomena of high importance to RBMK safety including water discharge, reflood, propagation of wetting front under nominal power.

The aim of chosen six experiments was to study temperature mode of the RBMK-1500 FA model under sharp decrease in coolant flow rate right down to its total termination (at high power generation) followed by its recovery. A similar situation can take place in the FC of the reference RBMK when MCP’s pressure header breaking. In this case all the group distribution headers connected to the pressure header are cut off by the check valves, which are installed at the inlet to these group headers. Water ceases to be delivered into the fuel channels. There begins steam filling in the channels. To prevent FA overheating, ECCS water is supplied into the core. In the first second after breaking, the reactor emergency protection system is actuated with signal on pressure increase in the rooms where pipelines are.

2. DESCRIPTION OF RBMK LOOP MODEL ON KS TEST FACILITY

The KS facility simulates the main forced circulation loop of an RBMK primary circuit.

KS RBMK Loop model (Figure 1) includes models of all the main elements of the RBMK main forced circulation circuit (FMCC) including: (1) pressure header (PH), (2) group distribution header (DH), (3) lower water communication lines (LWC), (4) an isolating control valve (ICV), (5) a full-size fuel channel (FC) with (6) an electrically heated fuel assembly (FA), (7) the lifting path with (8) assembly suspension, and (9) steam water communication lines (SWC). The SWC horizontal section has a slope of 0.7° . The upper horizontal header (10) and three vertical separators (11) do not model real drum separators (DS) but provide boundary conditions in the circuit outlet.

The model of RBMK-1500 reactor fuel assembly includes 18 fuel element simulators made of stainless steel tubes of 13.5 mm OD and a central unheated rod (OD 15 mm) of the same steel. The radial power peaking in the fuel assembly is provided due to differences in wall thickness of the heated tubes: wall thickness of 12 tubes in the peripheral row is 4 mm and that of 6 tubes in the inner row is 3 mm. The FE power in the peripheral row is higher than that in the inner row being proportional to the ratio of cross section areas of FE simulator tube walls (~ 1.21), and it correlates as 1.061 to 0.878, if 1 is the average FE's power. The fuel assembly model is heated by the direct current passing through the fuel element simulators with uniform power density distribution along the FA height. Cable thermocouples of 1.5 mm OD are sealed in the fuel element simulator walls.

Eleven RBMK-1500 reactor spacing grids-intensifiers with the full number of cells with pitch of 360 mm were installed in the upper part of the heated section along 3600 mm length. 20 grids-intensifiers of RBMK-1500 reactor were placed between them with 120 mm pitch, which served as spacers only for 6 fuel elements of the inner row. Nine authorized standard grids with 360 mm pitch were mounted in the lower part of the FA model.

The RBMK-1500 channel design differs from that of RBMK-1000 by spacer grids, which are equipped with heat exchange intensifiers in the FA upper part. Availability of these intensifiers in the upper part of the FA allows increasing in channel heat power.

The lower halves of RBMK-1500 and RBMK-1000 fuel assemblies are identical. Therefore some experimental results obtained in these experiments concerning the lower assembly half are applicable for RBMK-1000 (for instance, dryout onset, post dryout heat transfer...).

There is also an equipment that simulates operation of reactor drum separators (DS), steam condensers, downcomers and main circulation pumps of the RBMK primary circuit. However this equipment do not model the appropriate RBMK FMCC components. For this reason the RBMK primary circuit model at KS test facility is considered as semi-integral one.

Processes in the parallel fuel channels are under consideration during these experiments. One of the channels is considered as a full-size model of RBMK fuel channel. Impact of the rest parallel channels is simulated with the bypass (18). A great flow rate through the bypass provides constant pressure drop between the upper and lower headers in the course of the experiments.

The pressurization system used in the experiments includes 6 pressurizers of 0.52 m^3 in total volume connected to the 1-st collecting header. Nitrogen was used by way of gas medium.

More detailed description of RBMK MFCC model at the KS test facility is in [2].

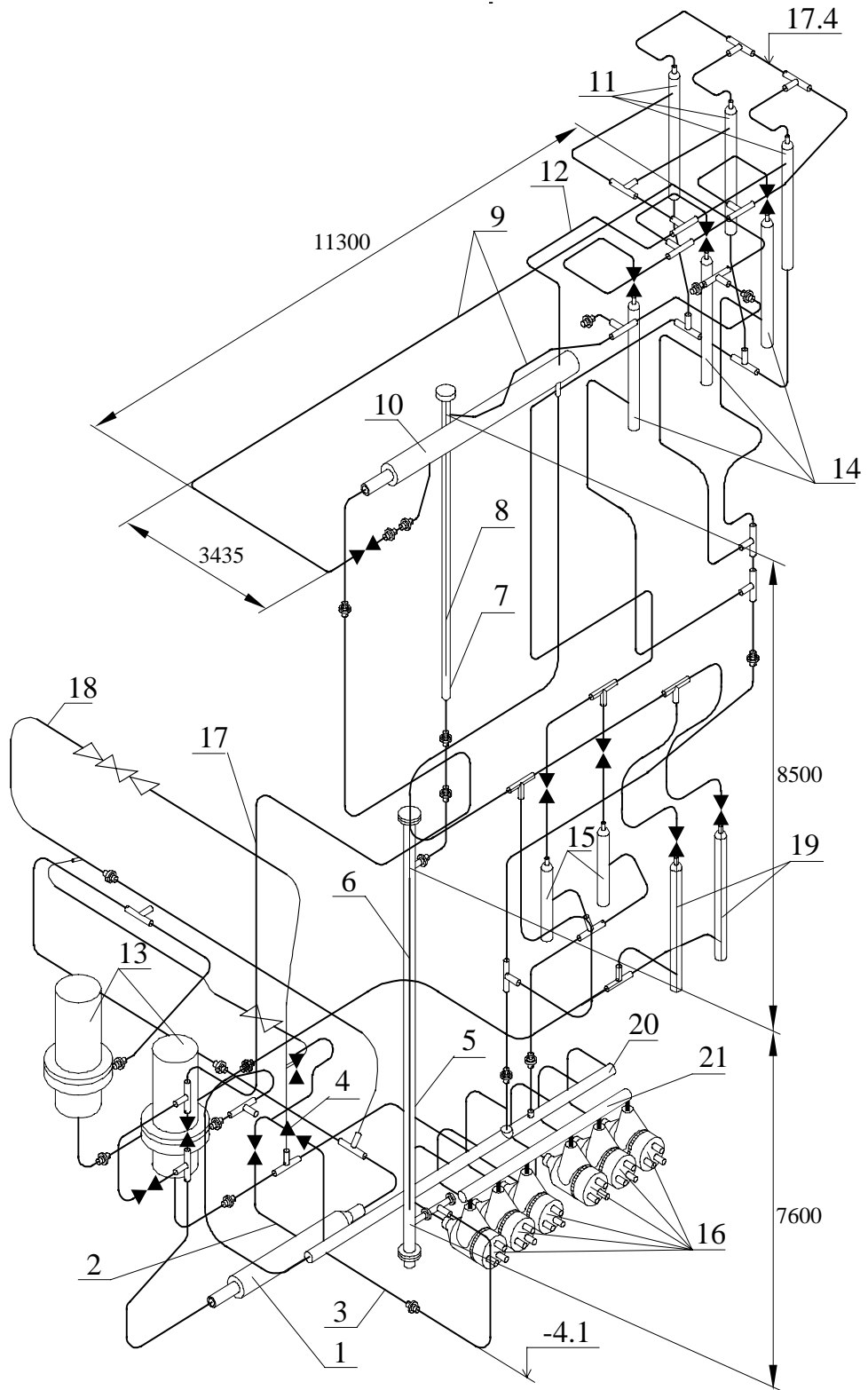


Figure 1. KS RBMK Loop model as used in the tests with a RBMK-1500 FA model.

3. TESTS DESCRIPTION

The FC model conditions during the experiments are nearly close to those when breaking the MCP’s pressure header in the RBMK reactor and cutting off fuel channels with check valves. When limiting temperature is reached on the fuel rod simulator surface there is resumption of flow rate through the fuel channel. Thus coolant circulation recovery on account of ECCS operation was simulated. Emergency protection system actuation was simulated by FA electrical power decreasing in only one experiment 5’. The rest experiments are carried out at a constant electrical power.

Processes/phenomena occurred in the RBMK FC model under sharp decrease in coolant flow rate right down to its total termination (at high power generation) succeeded by its recovery that were analyzed in computations were the following:

- water release from the FC model and fuel simulator surface drying,
- dryout under sharp flow deceleration at the inlet of the RBMK-1000 and RBMK-1500 FA models,
- post dryout heat transfer and fuel simulator temperature conditions in the FA model under channel drying,
- steam and water counter current flows in steam-water piping and in the FC with FA model,
- propagation of the reflood and quench fronts in FA model under flow resumption at the channel inlet.

Before beginning each experiment, the initial steady state with coolant forced circulation was set at given initial parameters outlined in Table 1.

Table 1. Parameters of the initial steady states for chosen six experiments.

Designation of experiment in [2]	N kW	G Kg/s	P _{in} MPa	T _{in} K	ΔP ₁₆₋₄ MPa
4	1691	3.90	7.68	516.1	0.1831
5	2486	4.70	8.40	527.4	0.2616
5’	2532	4.17	7.95	533.1	0.2715
6	2926	4.28	8.23	527.3	0.2714
7	3488	4.13	8.23	529.3	0.3107
8	4566	6.27	8.74	531.1	-

Coolant been supplied from the pumps went up through the riser of the fuel channel model and also through the bypass up to the upper header and then descended through four downcomers of RBMK FMCC model down to the suction side of the pumps.

Upon achieving steady state, parameter recording began and valve 2r at the inlet to the FC model (Fig. 1) closed completely and rapidly (during 3 s) causing decrease in coolant flow rate down to zero. At achieving predetermined limit temperature of fuel element simulators (this temperature mustn’t be more than 870 K), valve 2r quickly opened and coolant flow rate recovered. In this case, temperature of the fuel element simulators decreased down to that close to saturation one.

During transients, flow rate through the bypass remained practically constant (about 33.3 kg/s within the limits of experimental error). In the course of the experiments pressure in the upper header and separation columns was not maintained constant.

During one of the experiments (experiment 5'), the FA model electrical power was slowly decreased on closing valve 2r.

In the course of the experiments the following parameters were measured and registered:

Parameter	Absolute measurement error
FA model electrical power N	± 60 kW
Water mass flow rate G at the FC inlet	± 0.14 kg/s
Pressure P at the FA model lower part	± 0.15 MPa
Pressure drop ΔP_{16-4} on the FA model height	± 0.1 KPa
Water temperature T_{in} at the FA model inlet	± 6 K
FE simulator wall temperatures $T_{w1} - T_{w4}$ along the height of the FA model	± 16.5 K

The range of non-sensibility of the differential pressure gage is 0 - 120 KPa, because the device for measuring the pressure drop DP16-4 reached its lower measurement limit equal to 120 KPa.

According to special tests, response time of the thermocouples was 0.3 s.

4. RELAP5 MODEL AND ASSUMPTIONS

When calculating and assessing suitability of the code and its modeling units for description of separate phenomena and complex processes, it is conventional in the first stage of calculation to use the options recommended by the code developers for actuating the code models under analogous conditions. The general modeling approaches recommended in the RELAP5 manuals should continue to be used.

In the first stage, the following assumptions were made:

- Volume Vertical Stratification, Water Packing, Abrupt Area Change, Branching, Noncondensables, Umbrella Model were process models activated for the corresponding circuit components;
- process models such as an additional model of countercurrent flow limitation (CCFL Model), model of critical flow rate (Choked Model), and Reflood Model were not to be used in the corresponding circuit components.

To describe interphase friction in the coolant in the FC model with the FA, an option designating to rod bundle (with flag b=1) is applied. Semi-implicit scheme of numerical integration specified with the tt=3 option is used to calculate conjugate hydrodynamics and heat transfer/conduction processes.

In the second stage, when analyzing sensitivity, other necessary or additional phenomenon models and nodalizations can be used for better understanding.

RELAP5 model simulates the RBMK Loop model at the KS test facility. This model includes a riser being investigated that contains two branches with models of the main MFCC components, and auxiliary downcomer of four branches including components that ensure initial and boundary conditions in the MFCC part under consideration and also the test facility operation as a whole. Nodalization scheme for the RBMK MFCC model at the KS test facility (in terms of RELAP5) is presented in Figure 2. This nodalization scheme and input decks were developed with regard to the main assumptions when carrying out computer analysis of the tests.

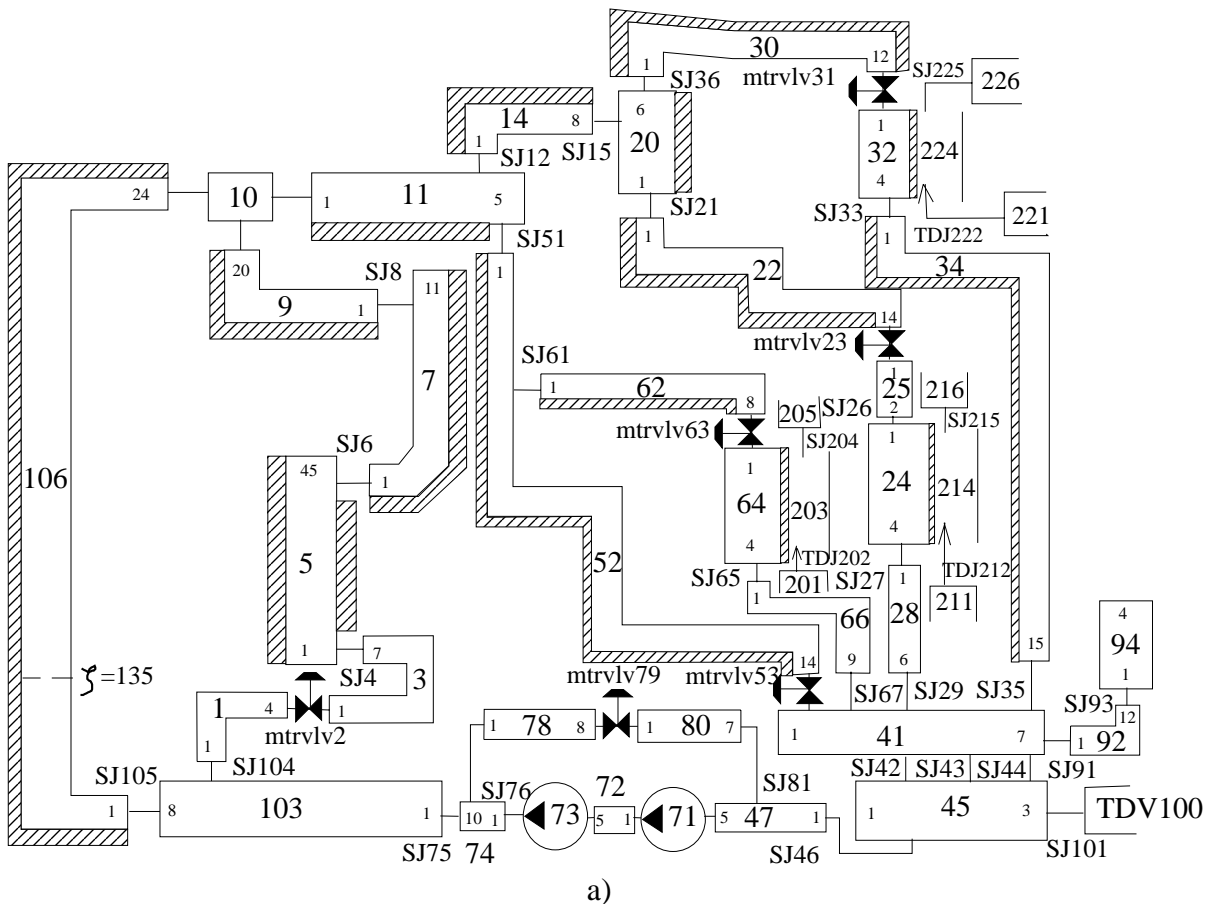


Figure 2. Nodalization scheme of RBMK Loop model at KS test facility:
a) KS RBMK Loop model,
b) Fuel channel model.

Taking into account a great quantity of components in the primary and secondary circuits of the KS test facility, it was used only one equivalent component when modeling each appropriate group of the typical components located in four branches of the downcomer. In particular, only one component vol.20 is used to simulate three separators (11). Three condensers (14) are modeled with one component vol.32. When developing these equivalent models, particular attention was given to parity between real volumes and lengths of inlet and outlet pipelines and those of corresponding hydrodynamical components as well as between surface areas of heat transfer toward water in the second circuit. This condition is necessary to bring about representation of experimental conditions of heat exchange between primary and secondary circuits and to ensure simulation of coolant pressure behavior in the primary circuit at transients under investigation. To do this the modeling of circuit volume sections with two-phase mixture and gas must be obviously suitable.

Coolant flow termination to FC model inlet with its successive resumption is simulated with closing and next opening of Valve 2r that uses a component like “motor valve 2”. To control valve “close” and “open” procedures at given time moments Trip Input Data are used.

When modeling the section of the fuel channel with the FA model it was chosen a fine nodalization for hydrodynamical components and heat structures along the channel length that was connected to the pitches between spacer grids and grid-intensifiers. To account the heat exchange processes to be impact by the grids, it were used “Additional Right Boundary Cards”.

In the early “base case” calculations, power density distribution in the fuel rod simulators over the FA cross section was uniform. Power of 12 rods in the peripheral row was underestimated by 6% lower than the experimental values, because the real radial power peaking factor of the FA model was 1.061. In this case there is also an overestimation of the power of 6 rods in the internal row with regard to the experimental values. This fact should be taken into consideration when comparing with experimental data. The rod simulator wall is portioned in thickness into 4 layers so that the external layer thickness is 0.75 mm corresponding to the deepness at which the thermocouple’s hot junction is positioned in the wall. This enables a direct comparison of calculation results of wall temperature at this depth with the experimental data on temperatures Tw1, Tw2, Tw3, and Tw4.

Channel walls of the riser and descending circuit sections to the points of the condenser, heat exchanger and aftercooler were also modeled with “heat structure” components in order to simulate heat accumulation in the metal and external heat losses.

5. THE RESULTS OF THE CODE ASSESSMENT

5.1. To estimate suitability of computer modeling of thermal hydraulic processes in the FC with FA model at the steady states for experiments the “base case” calculation results of the full pressure drops DP16-4 and rod temperatures across the FA model height were used.

In the steady states when decreasing in FA power the code leads to a systematic underestimation in pressure drops DP16-4 relating to the measured values. At FA power been equal to 1691 kW this underestimation is 22.5 %. With increasing in FA power the agreement between the calculated and experimental values of the pressure drop becomes better. Their coincidence is reached at FA power been equal to 2926 kW.

In the base case calculations the fact that 4 of the 5 steady-state DP16-4 (t) cal pressure drops are outside of the measurement error range is disturbing. The fact that 3 of the 5 pressure drops are below the measured values, and 1 of 5 pressure drop is above the measured one is likely indicative of a systematic error in modeling the losses in the test section (e.g., wrong friction factors). A similar behavior was noted in the base cases of the analysis of Standard Problem INSCSP-R1.

These discrepancies for full pressure drops DP16-4 at reduced values of the power may be resulted from the inaccurate code description of the local losses of pressure on the spacer grids and grid-intensifiers as well as wall and interphase frictions in the two-phase flow in the heated rod bundle. There needs to be some effort to address this error via parametric changes in the input. Therefore, sensitivity studies were performed with different FC wall roughness for experiments 4, 5, 5', 6, 7.

The calculated values of rod temperatures along the FA height are in satisfactory agreement with the experimental data at FA power ranged from 1691 to 3488 kW. In steady states the code describes with reasonable suitability the heat transfer in the two-phase flow in the channel with the RBMK-1500 FA in these experiments.

However at FA power equal to 4566 kW the code predicts a premature dryout at the end of the heated region (see Tw1 and Tw2) in the areas of high void fractions whereas there is no dryout in experiment 8. The reason for the considerable differences may be an inaccurate description of the critical heat flux at the high heat loads and great void fractions.

5.2. RELAP5/MOD3.2 describes with reasonable and minimal suitability the complex processes at the 1-st stage of the transients in the experiments with the constant FA power when the coolant flow rate decreases and completely terminates.

In particular, the pictures of the experimental and calculated pressures $P(t)$ are in a qualitative agreement, although at certain regime stages the calculated are essentially higher or lower than those measured in the transients. At the same time, the rates of increase or decrease in pressures dP/dt as well as finally achieved pressure values are essentially different from those obtained experimentally.

Predicted patterns of behavior of full pressure drop $DP_{16-4}(t)$ are in a qualitative agreement with the experimental data, although calculated values $DP_{16-4}(t)$ are essentially lower than their measured values.

The reasons for these discrepancies when describing the 1-st stage of transients may be as follows:

- non-adequate code description of dynamical processes of steam generation in the FC with FA as well as steam condensation in the components of the closed circuit as a whole and, consequently, non-adequate description of pressure behavior in the primary circuit and in the FC;
- inaccurate description of the interphase friction and interphase heat-exchange processes under conditions of the sharp decreasing and full termination of the flow rate at the FC inlet and, as a result, non-adequate code simulation of the saturated water flash boiling, water release from the channel with FA and then subcooled water flowing down (backwards) as well as dynamics of channel drying.

5.3. RELAP5/MOD3.2 reasonably describes *the influence of the constant FA power* on the character and rate of the thermal and hydrodynamic processes as well as on behavior of the parameters concerned in the 1-st stage of the transients (*type 1*).

The picture of the dryout initiation and its propagation along the FA height in experiments 4, 5, 6, and 7 (*type 1*) is described by the code with a reasonable or minimal suitability.

To assess integrally an accuracy of the code simulation of the complex processes, the dependence of time interval Δt_d (from the moment of full stop of flow rate to the beginning of increase in wall temperature $T_{w1}(t)$ at the FA outlet) upon FA power was used. The values of time intervals $\Delta t_d = t_d - t(GO)$ been predicted for experiments 4, 5, and 6 exceed their experimental values Δt_d by about ~1.6 s, 1.0 s, and 1.0 s, respectively. This excess of calculated values Δt_d over those obtained experimentally decreases and the pictures of the dryout initiation and its propagation along the FA height become more resembling in experiment 7.

This indicates a reasonable or minimal suitability of the simulation of the dryout initiation and its propagation along the FA height during the 1-st stage of the regime in the 1-st type experiments. The computation results would be still closer to the experimental data when simulating the radial heat release distribution in the FA model to be non-uniform and the flow rate behavior at the FC inlet as in reality.

5.4. The code describes with reasonable suitability the influence of FA power on the distribution of post dryout heat transfer and behavior of rod temperatures along the FA height at the channel drying. It is shown that the rod wall heating rates dT_w/dt at the FA outlet increase with increasing FA power.

It should be specially noticed that the maximum values $T_w(t)_{max}$ cal of the calculated wall temperatures do not exceed the maximum experimental magnitudes $T_w(t)_{max}$ exp. It means that the

code would be likely to underestimate the maximum cladding temperature, which would be a non-conservative result from a safety perspective.

5.5. The code describes with reasonable suitability the conditions for the dryout initiation and its propagation along the FA height under dynamical conditions with simultaneous involving both thermal and hydrodynamic perturbations in experiment 5' *when FA power decreasing (type 2)*.

However when describing the post dryout heat transfer and rod temperature regime the code underestimates the heat transfer coefficients in the various cross-sections along the FA height. The maximal values of the calculated wall temperatures $T_w(t)_{max\ cal}$ exceed the experimental values of the maximal wall temperatures $T_w(t)_{max\ exp}$ by 20 – 60 K. Therefore the code suitability is assessed to be minimal when describing the post dryout heat transfer and rod temperature regime in experiment 5'. The reasons for these discrepancies when describing the 1-st transient in experiment 5' may be as follows:

- non-adequate code description of dynamical processes of steam generation in the FC with FA as well as steam condensation in the components of the closed circuit as a whole, and, consequently, non-suitable description of pressure behavior in the primary circuit and in the FC;
- inaccurate description of the interphase friction and interphase heat-exchange processes under conditions of the simultaneous flow rate termination at the FC inlet and decrease in power $N(t)$.

As a consequence, the code does not yield a suitable description of processes of steam generation and water release from the channel with FA as well as subcooled water flowing down – backwards – to the channel. All together, this influenced on accuracy of the calculations of steam flow rates over the channel with FA and heat transfer coefficient at the stage of the full flow rate termination at the FC inlet as well as drying of the channel with FA.

5.6. The reflood model does not behave in RELAP5/MOD3.2, therefore the second stage of the investigated transients in the experiments being analyzed was simulated under conditions when the special reflood model is not in usage. This allowed to make more exact the conditions for modeling the thermal and hydrodynamic processes as well as to estimate the necessity and importance of an additional special code model to be used for analyzing of the reflood.

The non-adequate or minimally adequate code simulation of complex processes at the first stage of transients does not allow exactly modeling the initial conditions for the second stage of transients.

The code gives only a qualitative agreement between the general pictures of behavior of the rod temperatures along the FA height at the repeated quenching in experiment 4. However, the code gives insufficient agreement with experimental data concerning the time characteristics and conditions of the rod surface quenching in the upper part of the FA. Shown is that the calculated velocity of quench front propagation is about 3 times less than that in experiment 4 at constant power $N=1691$ kW.

At higher FA powers in experiments 4, 5, 6 (*type 1*), the code gives only a qualitative agreement demonstrating a presence of rod surface quenching in the lower FA part in the cross-section where thermocouple T_w1 is installed. At the same time, the rest of the cross-sections been positioned above do not quench during the 2-nd stage when calculating these experiments.

For experiment 7 at power $N=3488$ kW, all the cross-sections along the FA height are not quenched during the 2-nd stage of the regime, which is not in a qualitative agreement with the behavior of all the rod temperatures been measured.

When analyzing the reflood under dynamical conditions in experiment 5' (*type 2*) there is a minimal agreement between the general behaviors of the rod temperatures along the FA height during the 2-

nd stage of the regime. However the quantitative behavior of the calculated rod temperatures as well as the calculated velocity of quench front propagation along the FA height are in significant contrast to those been measured in experiment 5'.

The analysis results obtained when modeling the reflooding of the RBMK-1000 and RBMK-1500 FC with FA allow the code suitability being assessed as insufficient. Shown is the necessity and importance of an additional special model (Reflood Model) to be used for suitable description of the 2-nd stage of transients. However, at validation of the advanced code version RELAP5/MOD3.2.2 and assessment of its additional reflood model, it will be necessary to achieve a suitable simulation of the initial conditions for the 2-nd stage of transients.

5.7. Sensitivity studies were performed with different FC wall roughness $4 \cdot 10^{-6}$ m and $4 \cdot 10^{-5}$ m in the FC model for experiments 4, 5, 5', 6 and 7 to estimate its influence on code simulation of complex thermal hydraulic processes in the FC. In steady conditions the increasing in FA power leads to a better agreement between experimental and calculated values of pressure drops DP16-4 across the FA model height with achieving good coincidence within the measurement accuracy for experiment 5 at FA power of 2486 kW. At the same time for experiments 5', 6 and 7, when FA power to be increased, the calculated values of pressure drops DP16-4 were evidenced to be systematically overestimated in reference to the measured values. Here, an increase in FA power leads to increase in discrepancy between calculated and experimental DP16-4 values. In steady state conditions the increasing of the FC wall roughness in 10 times results in code over prediction for DP16-4 pressure drops by 9.4, 15.6 and 28.0 % for experiments 5', 6 and 7 respectively. It is shown that increasing of the FC model wall roughness does not aid to reach better agreement with FC pressure drops in the experiments under higher FA power.

It is shown, the increased FA wall roughness weakly influences on the behavior of pressure drop DP16-4 (t), and also of the wall temperatures Tw1 (t), Tw2 (t), Tw3 (t), and Tw4 (t) during the 1-st and 2-nd stages for experiments 4, 5, 5', 6 and 7.

5.8. Using two lumped rod simulators ($Kr=1.061$) and accurate code description of the real flow rate behavior at the FC inlet (TDJ) gives more realistic code description of the initial and boundary conditions. The values of time intervals $\Delta t_d = t_d - t(G0)$ been predicted for experiments 4 and 5 exceed their experimental values Δt_d by about ~ 1.1 s and 0.2 s, respectively. This excess of calculated values Δt_d over those obtained experimentally decreases and the pictures of the dryout initiation and its propagation along the FA height become more resembling in these cases. This indicates a reasonable or minimal suitability of the simulation of the dryout initiation and its propagation along the FA height during the 1-st stage of the regime in the 1-st type experiments.

6. GENERALIZED CONCLUSIONS

The results of the code assessment (code performance for process/phenomenon) are presented in the following summary table.

<i>1. Process/Phenomenon in the steady states in the experiments 4, 5, 5', 6, 7, 8 with different FA power</i>	<i>Results of the code assessment</i>
1.1. Full pressure drop along the height of the channel with RBMK-1500 FA model	Minimal suitability
1.2. Heat transfer in the two-phase flow in the channel with the RBMK-1000 FA and RBMK-1500 FA models	Reasonable suitability
1.3. Dryout at the end of the RBMK-1500 FA heated region under high void fractions and the critical heat flux conditions	Minimal or insufficient suitability (exp. 8)

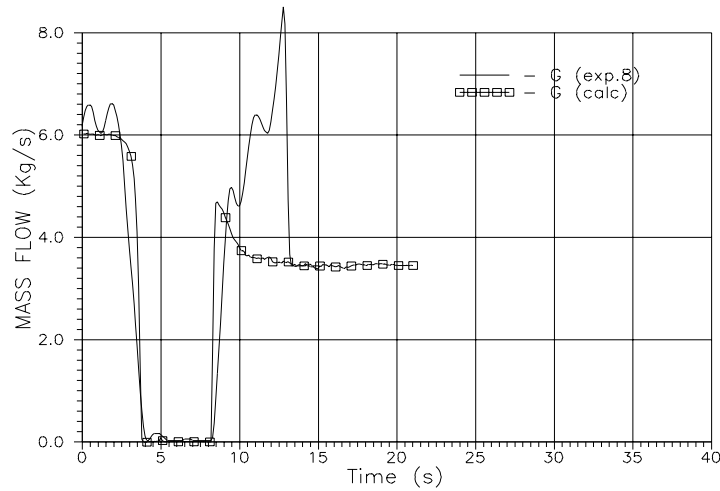
<i>2. Process/Phenomenon on the stage of decrease and full stop of coolant flow rate in the experiments 4, 5, 6, 7, 8 (type 1)</i>	<i>Results of the code assessment</i>
2.1. Water release from the FC model and fuel element surface dryout	Minimal suitability
2.2. Dryout under sharp flow deceleration at the inlet of the RBMK-1000 FA model	Reasonable and minimal suitability
2.3. Dryout under sharp flow deceleration at the inlet of the RBMK-1500 FA model	Reasonable and minimal or insufficient suitability (exp. 8)
2.4. Post dryout heat transfer and fuel element temperatures behavior in the RBMK-1000 FA and RBMK-1500 FA models under stop of flow and channel drying conditions	Reasonable and minimal suitability
<i>3. Process/Phenomenon on the stage of decrease and full stop of coolant flow rate in the experiment 5' (type 2) under dynamical conditions with simultaneous involving both thermal and hydrodynamic perturbations</i>	<i>Results of the code assessment</i>
3.1. Dryout under sharp flow deceleration at the inlet of the RBMK-1000 FA model	Reasonable and minimal suitability
3.2. Dryout under sharp flow deceleration at the inlet of the RBMK-1500 FA model	Reasonable and minimal suitability
3.3. Post dryout heat transfer and fuel elements temperature conditions in the RBMK-1000 FA and RBMK-1500 FA models under channel drying	Minimal suitability
<i>4. Process/Phenomenon on the recovery stage of water supply into the channel</i>	<i>Results of the code assessment</i>
4.1. Propagation of the reflood and quench fronts in the RBMK-1500 FA model under flow resumption at the channel inlet	Insufficient suitability

7. REFERENCES

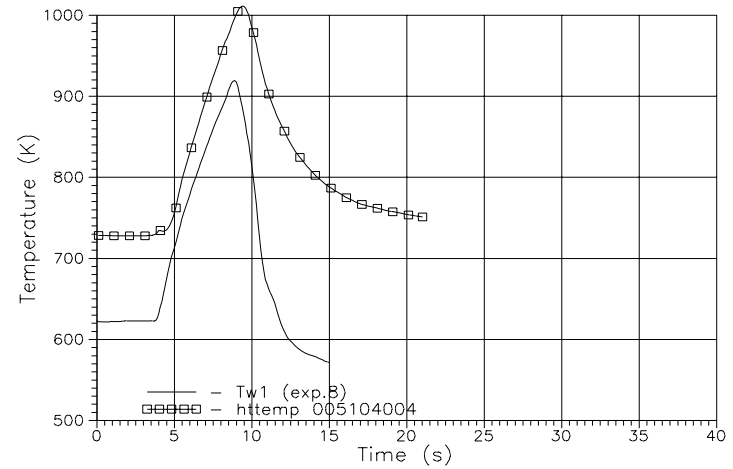
1. "Final RELAP5 validation plan for application to RBMK" , submitted as Deliverable 6 under Joint Project 6, phase 2 (Computer Code Validation for Transient Analysis of VVER and RBMK Reactors), International Nuclear Center of Russia Minatom, Moscow, Russia (January 1998).
2. Computer code validation for transient analysis of VVER and RBMK reactors: Standard Problem INSCSP-R2 Definition "RBMK tipe reactor core thermal hydraulic processes investigation under pressure header break conditions", Experiments with KS RRC KI test facility, International Nuclear Center of Russia Minatom, Moscow, Russia (August 1999).

Experiment 8, $N= 4566$ kW, $G_{in}=6.02$ Kg/s, $P_{in}=8.74$ Mpa, $T_{in}=531$ K

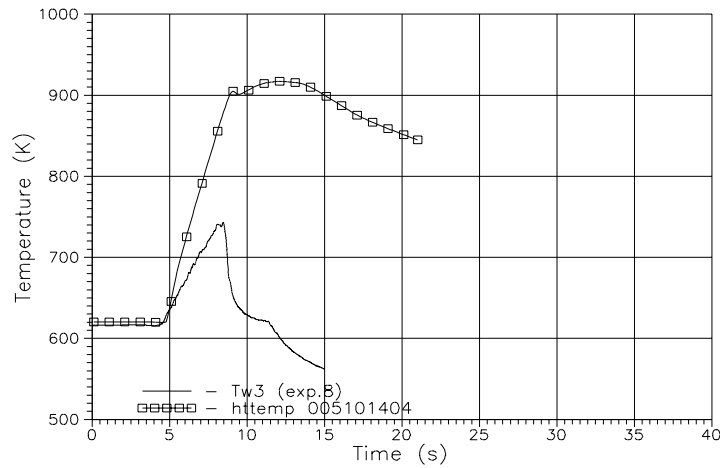
Base case: $Kr=1$, roughness $4 \cdot 10^{-6}$ m



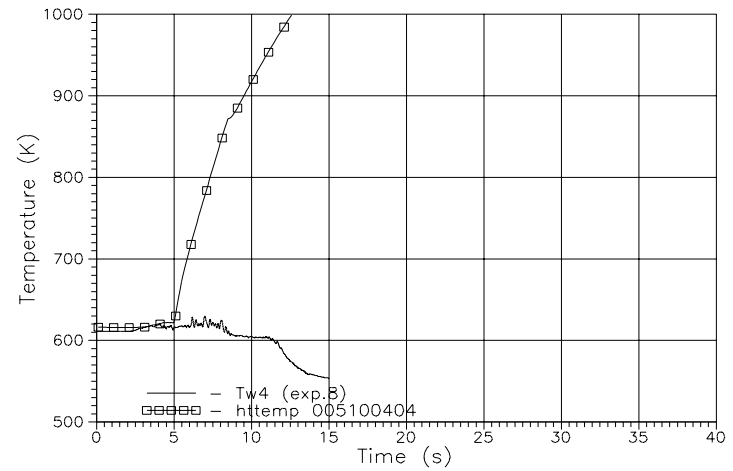
Mass flow rate G at the FC inlet



Wall temperature $Tw1$ ($z=6.94$ m)



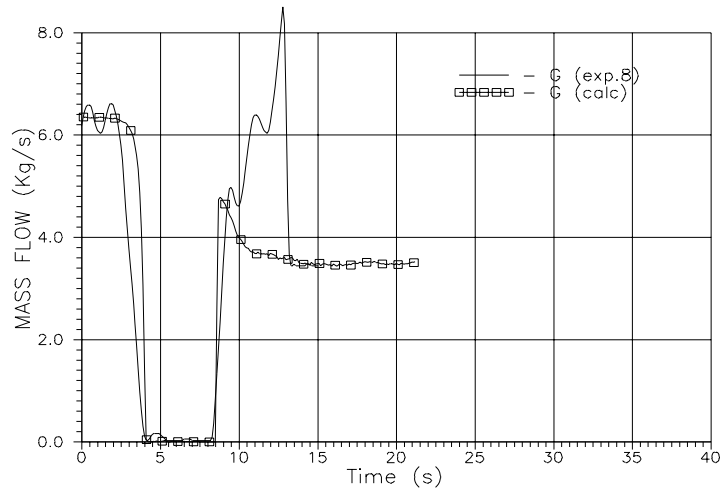
Wall temperature $Tw3$ ($z=3.82$ m)



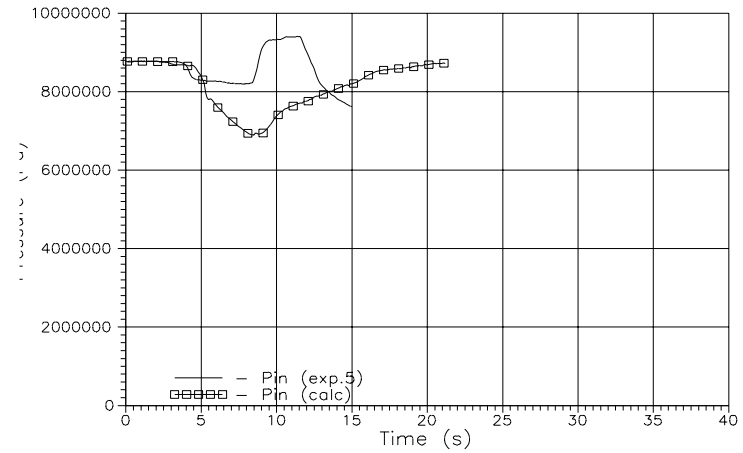
Wall temperature $Tw4$ ($z=1.04$ m)

Experiment 8, $N= 4566 \text{ kW}$, $G_{in}=6.35 \text{ Kg/s}$, $P_{in}=8.74 \text{ Mpa}$, $T_{in}=531 \text{ K}$

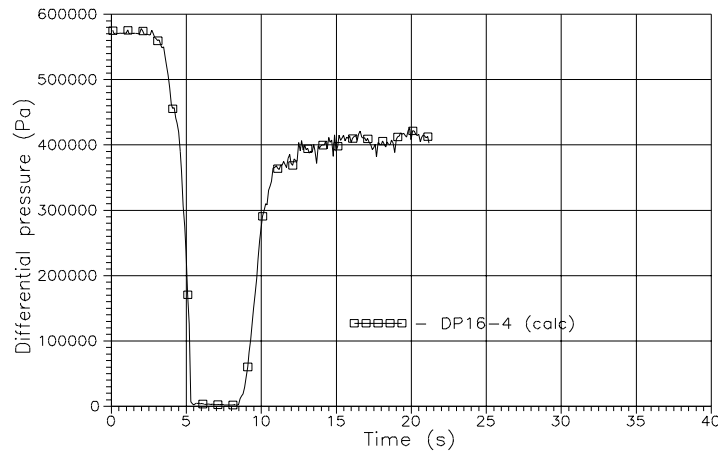
Base case: $Kr=1$, roughness $4 \cdot 10^{-6} \text{ m}$



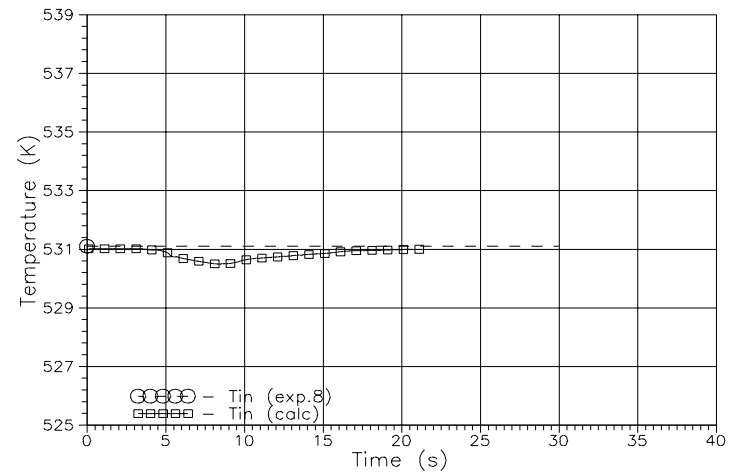
Mass flow rate G at the FC inlet



Pressure P in the lower part of FA

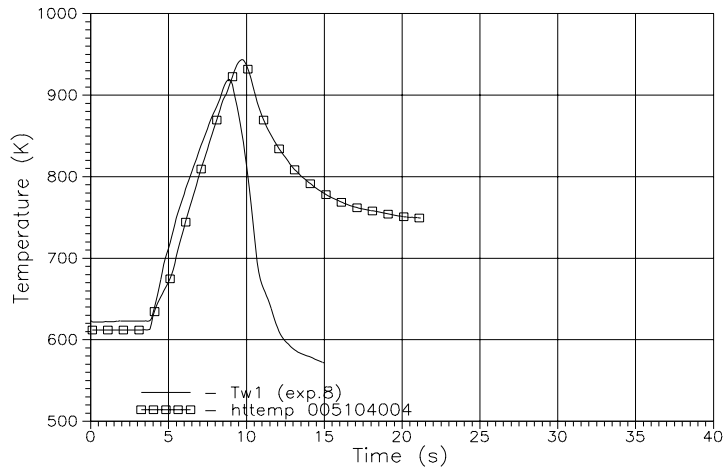


Pressure drop P_{16-4} along FA

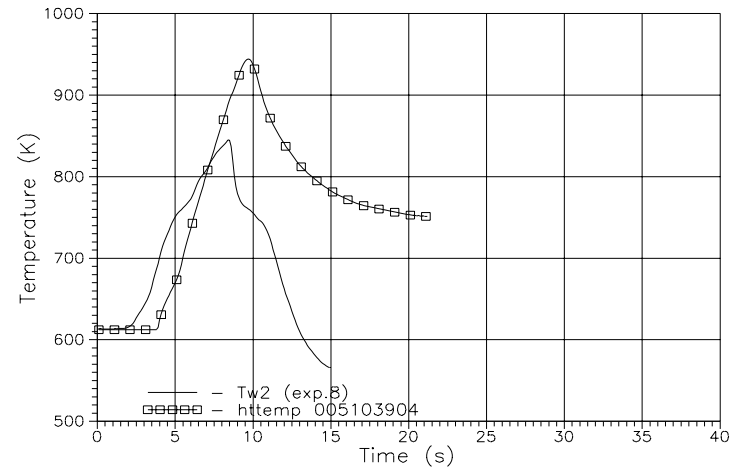


Coolant temperature T_{in} at the FC inlet

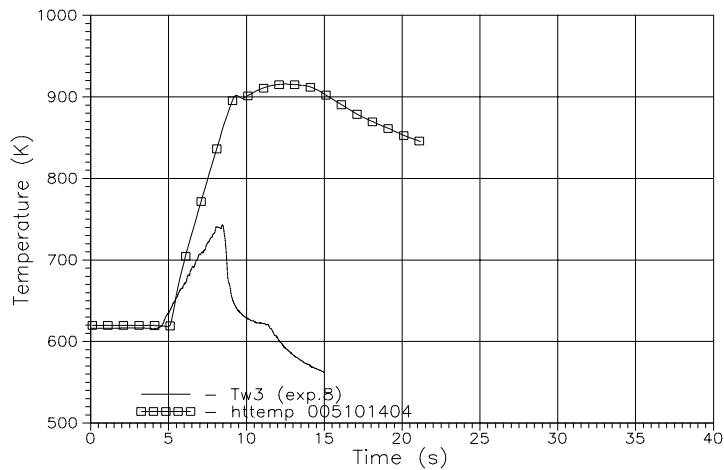
Experiment 8, $N= 4566$ kW, $G_{in}=6.35$ Kg/s, $P_{in}=8.74$ Mpa, $T_{in}=531$ K
Base case: $Kr=1$, roughness $4 \cdot 10^{-6}$ m



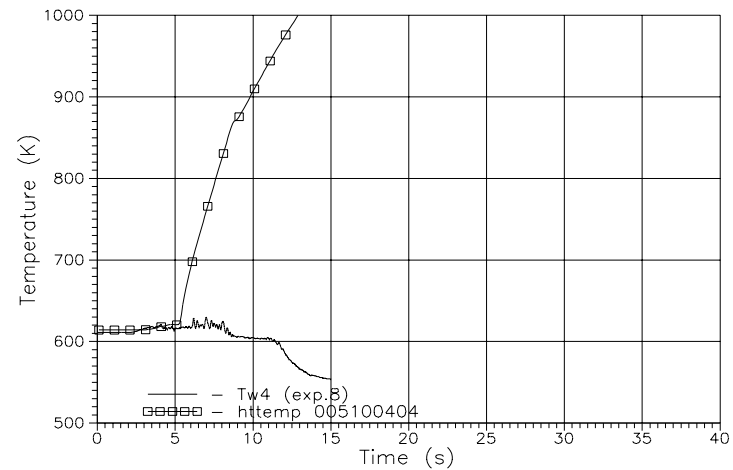
Wall temperature $Tw1$ ($z=6.94$ m)



Wall temperature $Tw2$ ($z=6.82$ m)



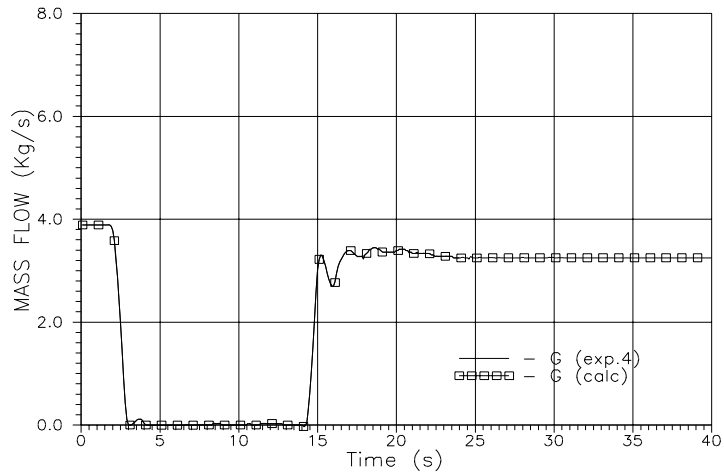
Wall temperature $Tw3$ ($z=3.82$ m)



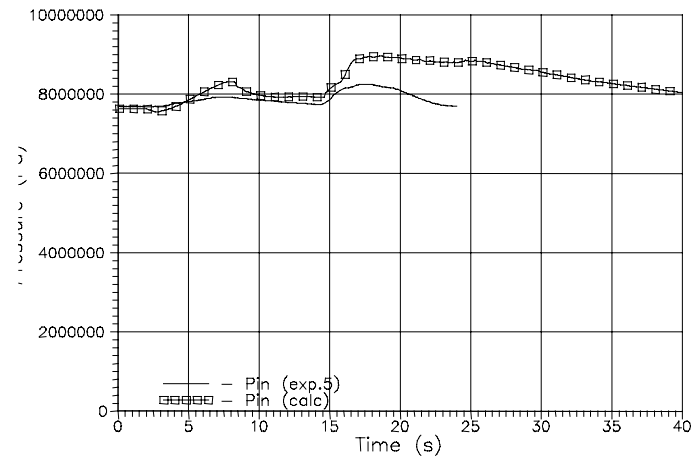
Wall temperature $Tw4$ ($z=1.04$ m)

Experiment 4, $N=1691$ kW, $G_{in}=3.90$ Kg/s, $P_{in}=7.68$ Mpa, $T_{in}=516$ K

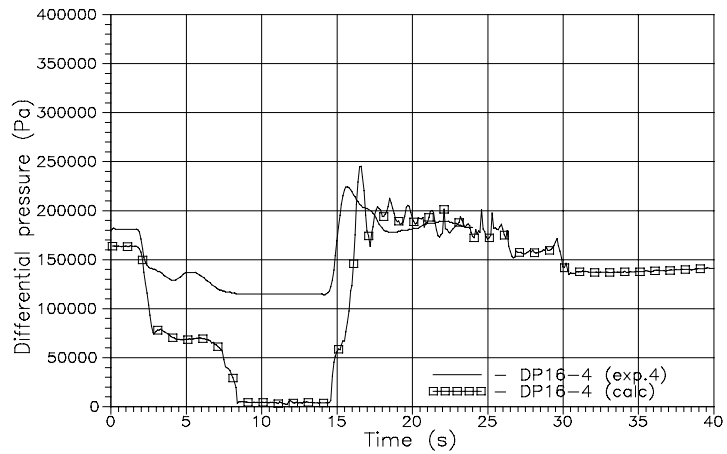
Sensitivity study: $Kr=1$, roughness $4 \cdot 10^{-5}$ m, TDJ



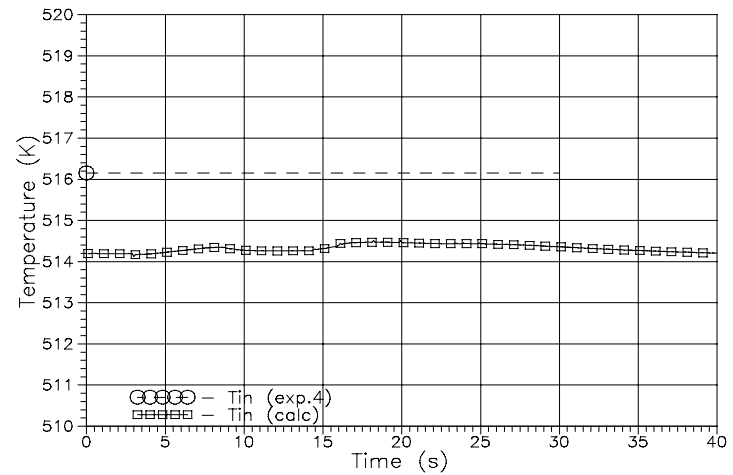
Mass flow rate G at the FC inlet



Pressure P in the lower part of FA

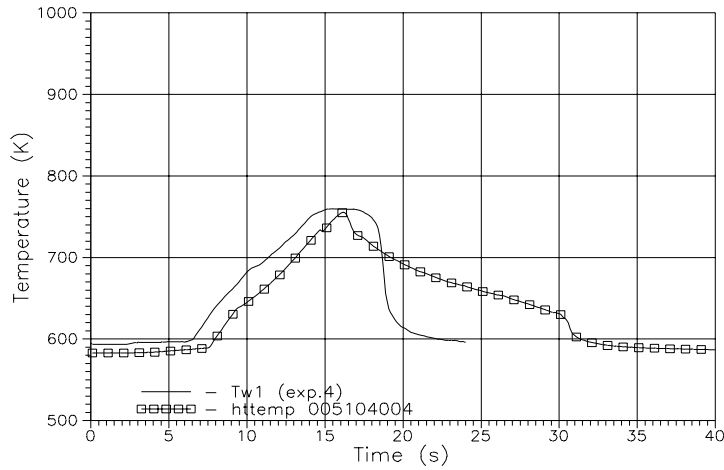


Pressure drop P_{16-4} along FA

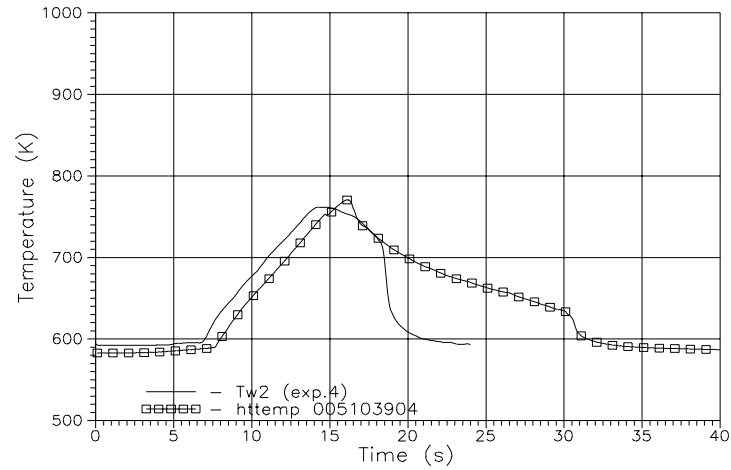


Coolant temperature T_{in} at the FC inlet

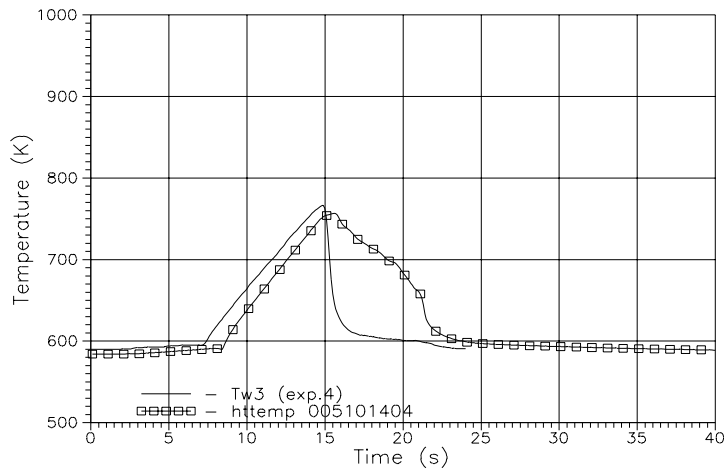
Experiment 4, N= 1691 kW, Gin=3.90 Kg/s, Pin=7.68 Mpa, Tin=516 K
Sensitivity study: Kr=1, roughness 4*10⁻⁵ m, TDJ



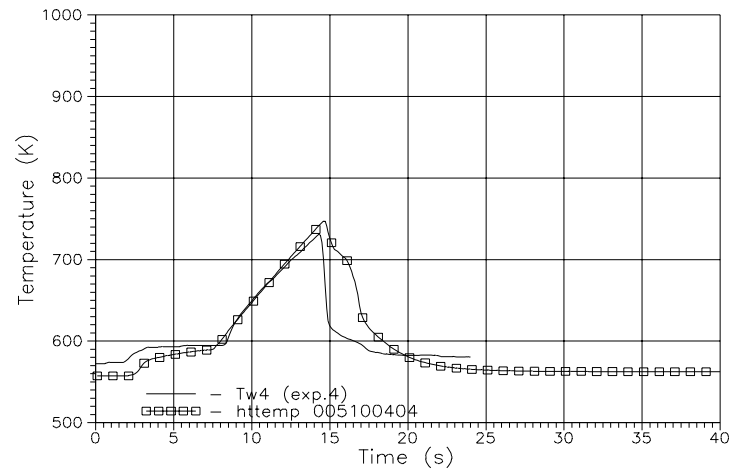
Wall temperature Tw1 (z=6.94 m)



Wall temperature Tw2 (z=6.82 m)



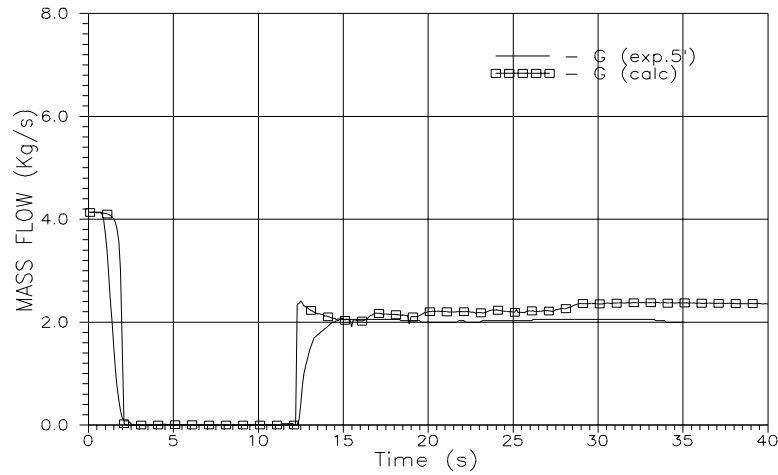
Wall temperature Tw3 (z=3.82 m)



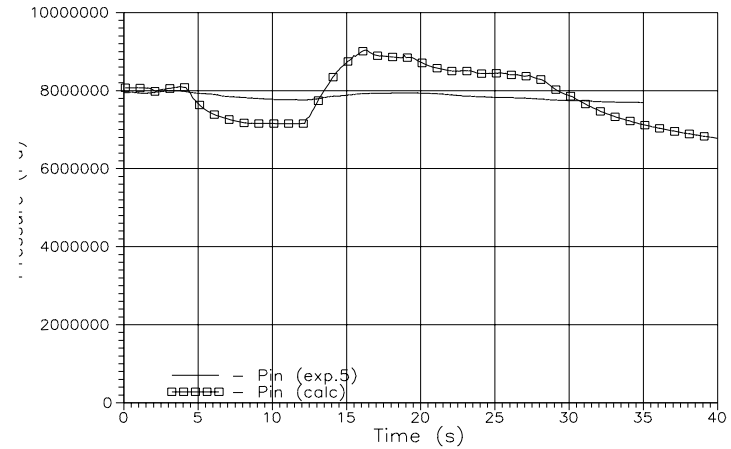
Wall temperature Tw4 (z=1.04 m)

Experiment 5', N= 2532 kW, $G_{in}=4.17$ Kg/s, $P_{in}=7.95$ MPa, $T_{in}=533$ K

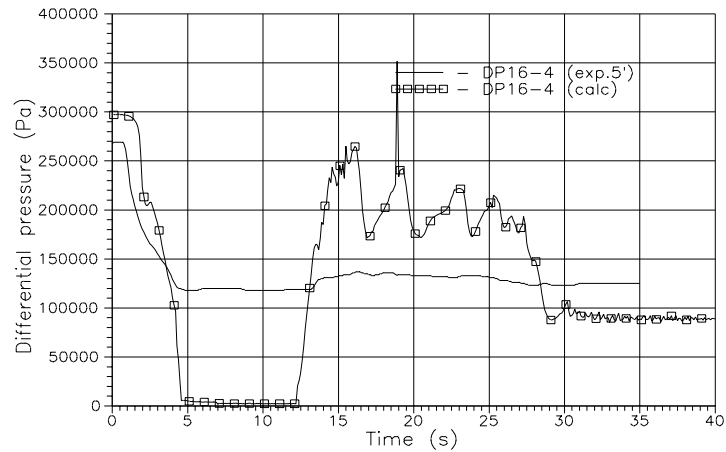
Base case: $K_r=1$, roughness $4 \cdot 10^{-6}$ m



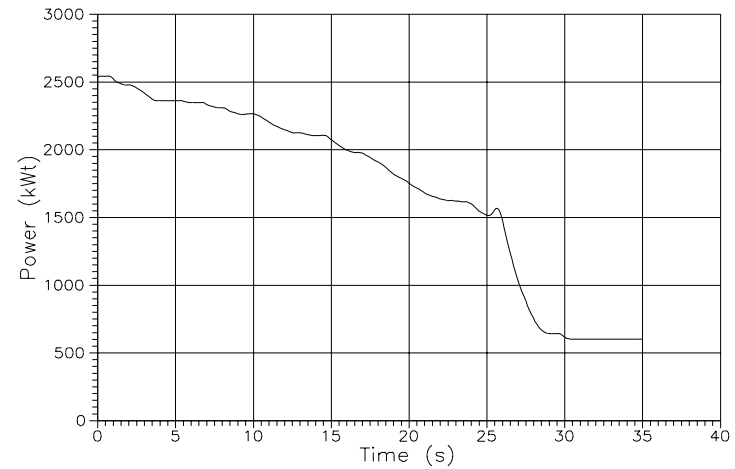
Mass flow rate G at the FC inlet



Pressure P in the lower part of FA

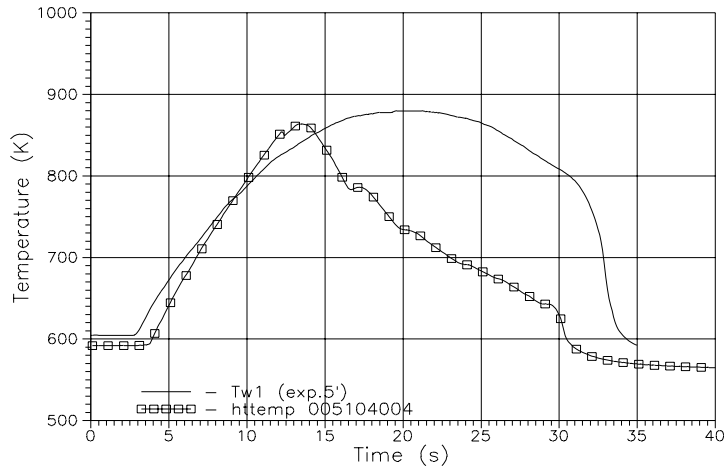


Pressure drop P16-4 along FA

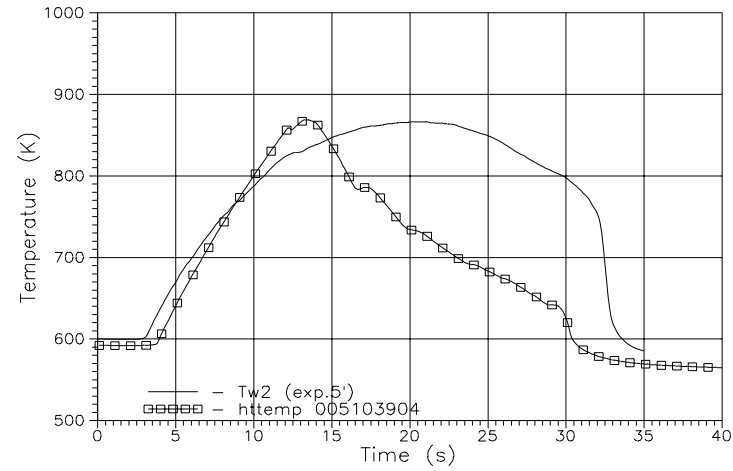


FC power history

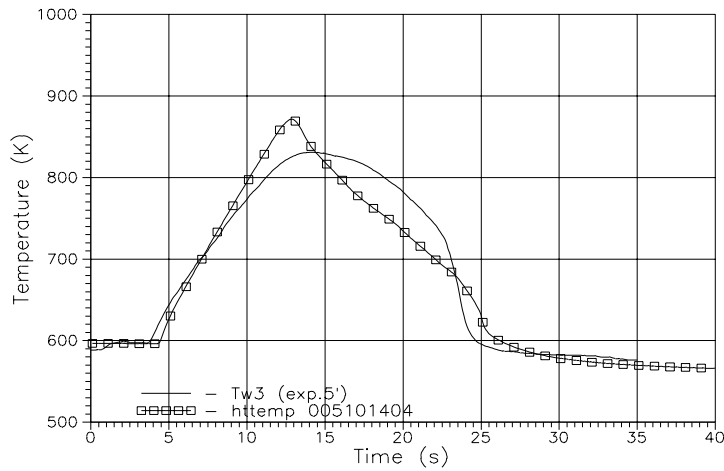
Experiment 5', N= 2532 kW, $G_{in}=4.17$ Kg/s, $P_{in}=7.95$ MPa, $T_{in}=533$ K
Base case: $Kr=1$, roughness $4 \cdot 10^{-6}$ m



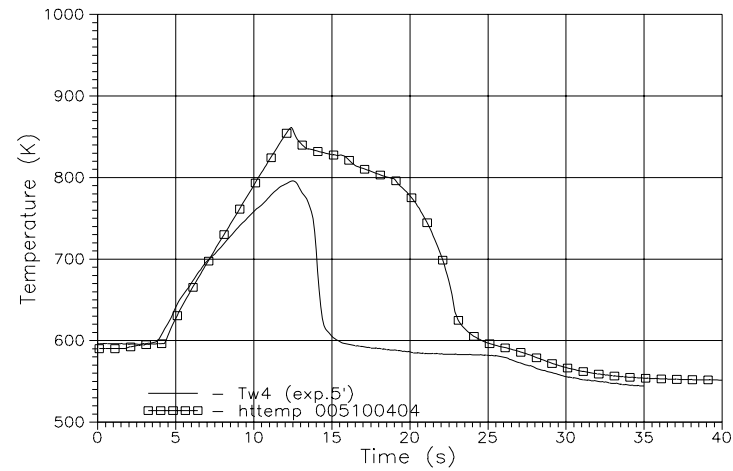
Wall temperature $Tw1$ ($z=6.94$ m)



Wall temperature $Tw2$ ($z=6.82$ m)



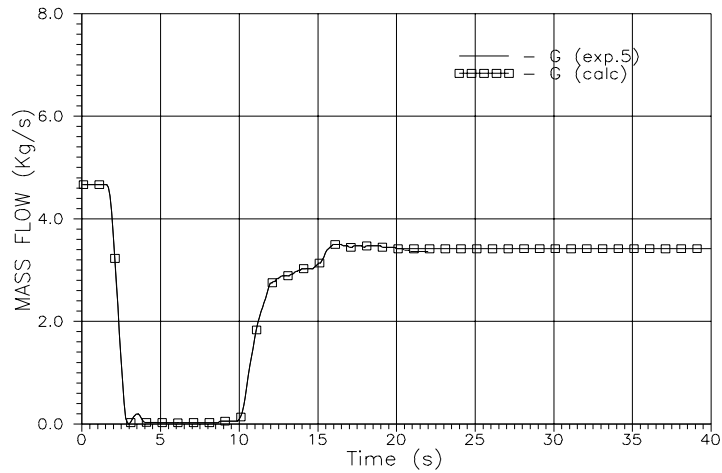
Wall temperature $Tw3$ ($z=3.82$ m)



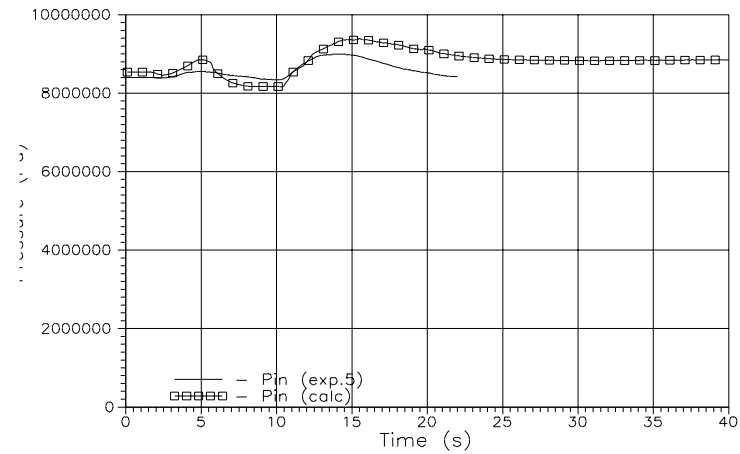
Wall temperature $Tw4$ ($z=1.04$ m)

Experiment 5, $N= 2486$ kW, $G_{in}=4.7$ Kg/s, $P_{in}=8.4$ Mpa, $T_{in}=K$

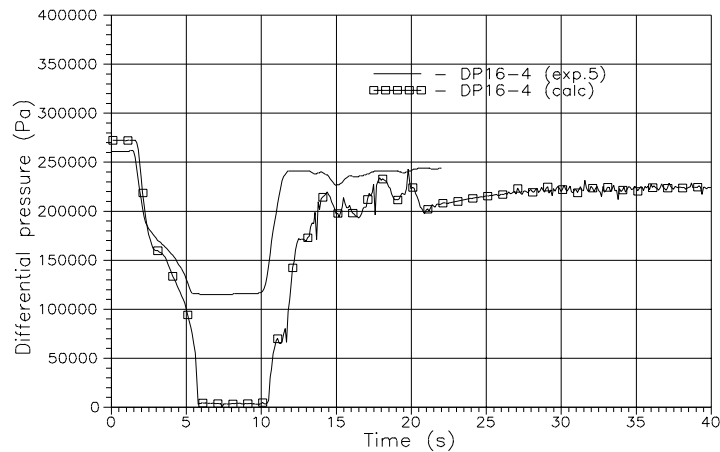
Sensitivity study: $Kr=1.061$, roughness $4*10^{-5}$ m, TDJ.



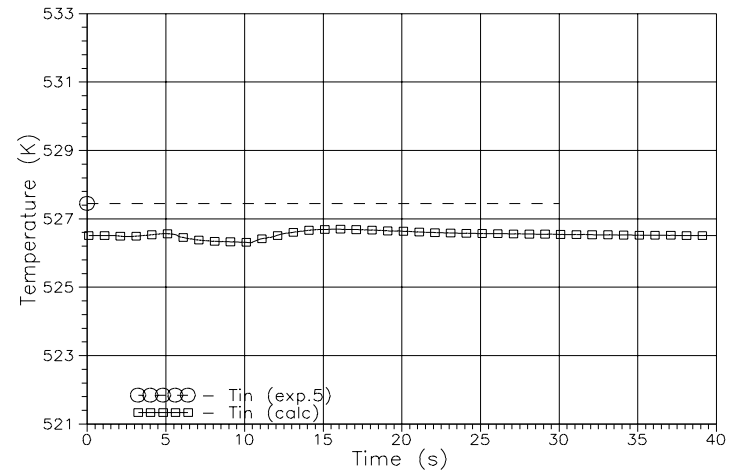
Mass flow rate G at the FC inlet



Pressure P in the lower part of FA

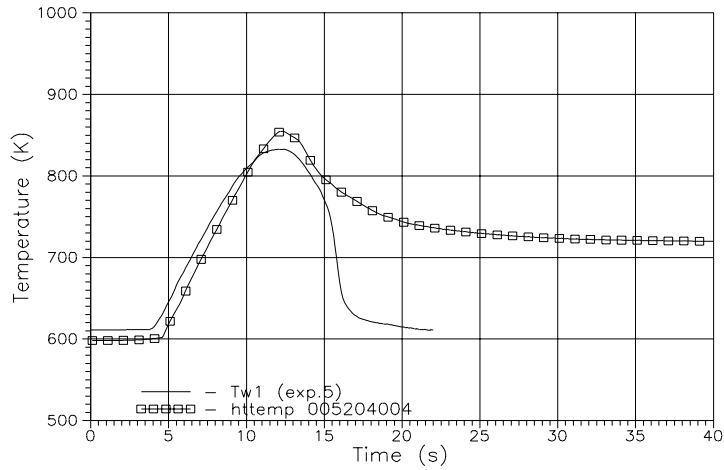


Pressure drop P16-4 along FA

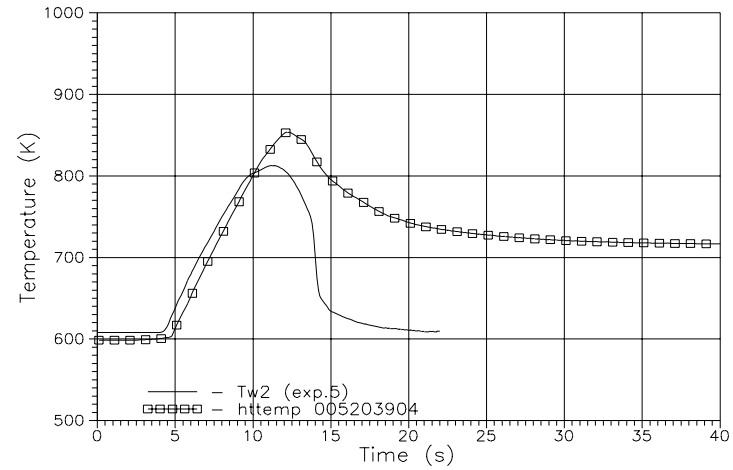


Coolant temperature T_{in} at the FC inlet

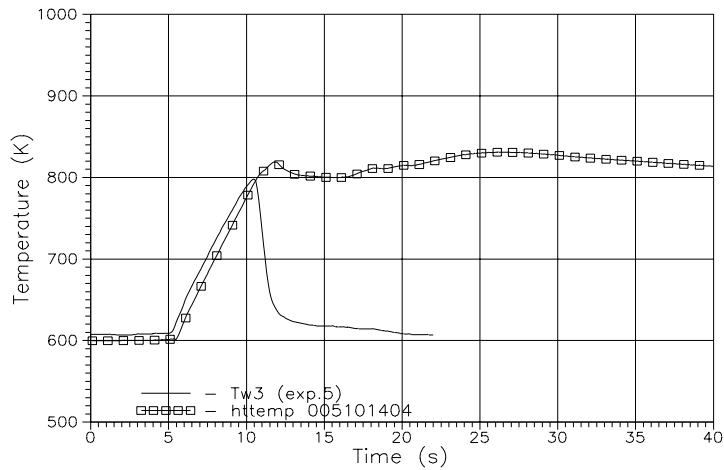
Experiment 5, N= 2486 kW, Gin=4.7 Kg/s, Pin=8.4 Mpa, Tin=K
Sensitivity study: Kr=1.061, roughness 4*10⁻⁵ m, TDJ.



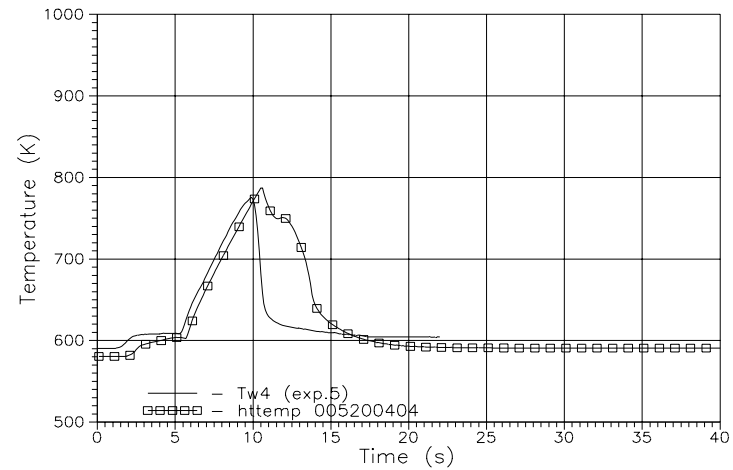
Wall temperature Tw1 (z=6.94 m)



Wall temperature Tw2 (z=6.82 m)

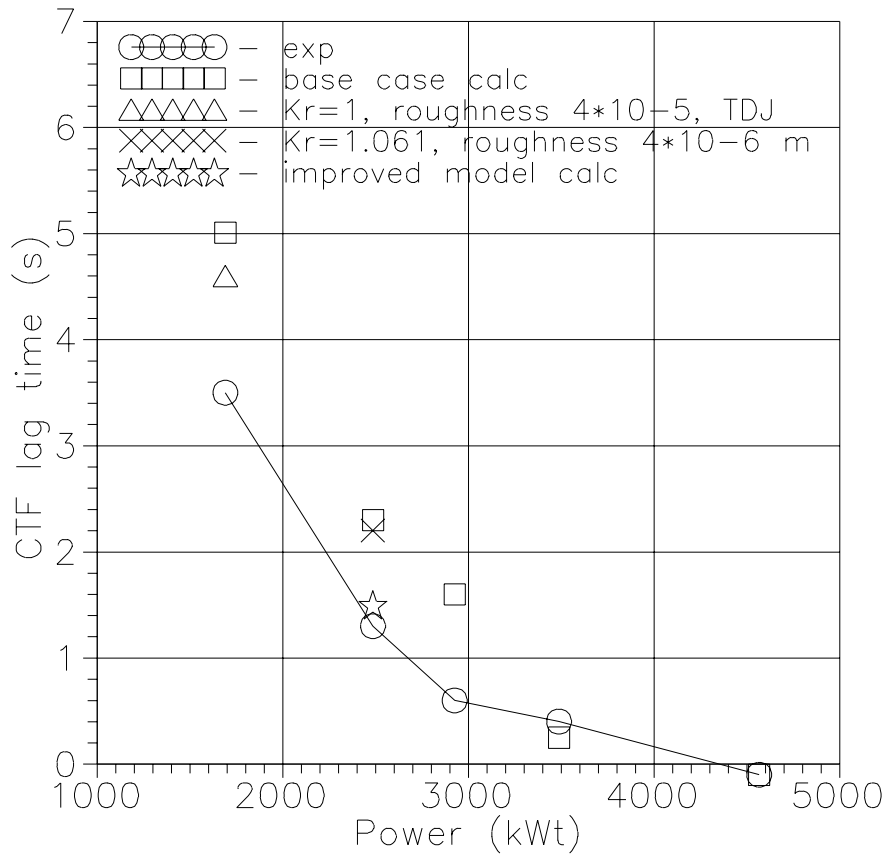


Wall temperature Tw3 (z=3.82 m)



Wall temperature Tw4 (z=1.04 m)

Sensitivity calculation results for the dependence of the time interval Δt_d on FA power.



Base case calculation: $Kr=1$, roughness $4 \cdot 10^{-6}$ m,
Motor Valve 2r

Sensitivity study: $Kr=1.061$, roughness $4 \cdot 10^{-6}$ m,
Motor Valve 2r

Sensitivity study: $Kr=1$, roughness $4 \cdot 10^{-5}$ m,
Motor Valve 2r

Improved model calculation: $Kr=1.061$,
roughness $4 \cdot 10^{-5}$ m, TDJ